Journal for ImmunoTherapy of Cancer

Endosialin-positive CAFs promote hepatocellular carcinoma progression by suppressing CD8$^+$ T cell infiltration

Lunbiao Gan ,[1] Tong Lu ,[2] Yu Lu ,[1] Hongtao Song ,[2] Jiayu Zhang ,[2] Keying Zhang ,[2] Shiqi Lu ,[1] Xinjie Wu ,[1] Fengze Nie ,[1] Sijia Di ,[1] Donghui Han ,[2] Fa Yang ,[2] Weijun Qin ,[2] Weihong Wen [1]

To cite: Gan L, Lu T, Lu Y, *et al*. Endosialin-positive CAFs promote hepatocellular carcinoma progression by suppressing CD8$^+$ T cell infiltration. *Journal for ImmunoTherapy of Cancer* 2024;**12**:e009111. doi:10.1136/jitc-2024-009111

► Additional supplemental material is published online only. To view, please visit the journal online (https://doi.org/10.1136/jitc-2024-009111).

LG and TL contributed equally.

Accepted 27 July 2024

[1]Xi'an Key Laboratory of Stem Cell and Regenerative Medicine, Institute of Medical Research, Northwestern Polytechnical University, Xi'an, China
[2]Department of Urology, Xijing Hospital, Fourth Military Medical University, Xi'an, China

Correspondence to
Professor Weihong Wen; weihongwen@nwpu.edu.cn

Dr Weijun Qin; qinwj@fmmu.edu.cn

Dr Fa Yang; yangfa0109@163.com

ABSTRACT

Background and aims Endosialin, also known as tumor endothelial marker1 or CD248, is a transmembrane glycoprotein that is mainly expressed in cancer-associated fibroblasts (CAFs) in hepatocellular carcinoma (HCC). Our previous study has found that endosialin-positive CAFs could recruit and induce the M2 polarization of macrophages in HCC. However, whether they may regulate other types of immune cells to promoting HCC progression is not known.

Approach and results The growth of both subcutaneous and orthotopic HCC tumors was significantly inhibited in endosialin knockout (EN^{KO}) mice. Single-cell sequencing and flow cytometry analysis showed that tumor tissues from EN^{KO} mice had increased CD8$^+$ T cell infiltration. Mixed HCC tumor with Hepa1-6 cells and endosialin knockdown fibroblasts also showed inhibited growth and increased CD8$^+$ T cell infiltration. Data from in vitro co-culture assay, chemokine array and antibody blocking assay, RNA-seq and validation experiments showed that endosialin inhibits the phosphorylation and nuclear translocation of STAT1 in CAFs. This inhibition leads to a decrease in CXCL9/10 expression and secretion, resulting in the suppression of CD8$^+$ T cell infiltration. High level of endosialin protein expression was correlated with low CD8$^+$ T infiltration in the tumor tissue of HCC patients. The combination therapy of endosialin antibody and PD-1 antibody showed synergistic antitumor effect compared with either antibody used individually.

Conclusions Endosialin could inhibit CD8$^+$ T cell infiltration by inhibiting the expression and secretion of CXCL9/10 in CAFs, thus promote HCC progression. Combination therapy with endosialin antibody could increase the antitumor effect of PD-1 antibody in HCC, which may overcome the resistance to PD-1 blockade.

WHAT IS ALREADY KNOWN ON THIS TOPIC

⇒ Endosialin is specifically expressed in cancer-associated fibroblasts (CAFs) in hepatocellular carcinoma (HCC). Endosialin-positive CAFs could promote HCC progression by recruiting and inducing the M2 polarization of macrophages. However, whether they may regulate other types of immune cells in HCC is not known.

WHAT THIS STUDY ADDS

⇒ We found that endosialin-positive CAFs could inhibit CD8$^+$ T cell infiltration by the inhibition of the expression and secretion of CXCL9/10 in CAFs, thus promoting HCC progression.

⇒ Combination therapy of endosialin antibody and PD-1 antibody showed synergistic antitumor effect compared with either antibody alone.

HOW THIS STUDY MIGHT AFFECT RESEARCH, PRACTICE OR POLICY

⇒ These results revealed a novel mechanism for how endosialin-positive CAFs promote HCC progression and will contribute to the development of novel combination therapy strategy for HCC, which may overcome the resistance to PD-1 blockade.

INTRODUCTION

Hepatocellular carcinoma (HCC) is the most common form of liver cancer and the third-leading cause of cancer mortality worldwide.[1 2] Current treatment strategies include surgical interventions, chemoembolization and systemic therapies. Although combined therapies, like immune checkpoint inhibitor (ICI) and tyrosine kinase inhibitors or anti-VEGF therapies, or even combinations of two immunotherapy regimens showed encouraging therapeutic effects in clinic, however, some patients still do not respond to any of these strategies.[3] Thus, more therapeutic strategies are still needed, and the elucidation of the molecular mechanisms that promote HCC progression will definitely help to develop novel therapeutic strategies.

Tumor microenvironment (TME) is composed of various cellular and acellular components including stroma cells, immune cells, blood vessels, extracellular matrix (ECM) proteins and plenty of secretory molecules.[4] Among them, cancer-associated fibroblasts (CAFs) are the most important component of TME in HCC since HCC develops almost exclusively in patients with chronic liver disease and advanced fibrosis.[5]

In HCC, CAFs are mainly derived from hepatic stellate cells (HSCs), and they can promote HCC progression through different mechanisms including promoting tumor cell proliferation, enhancing the stemness of HCC cells, stimulating tumor angiogenesis, inducing ECM remodeling, and contributing to the formation of immunosuppressive TME, *et al*.[6–8]

Because of their tumor-promoting function, CAFs have been considered as effective therapeutic targets for HCC treatment.[9–11] However, until now, no ideal surface marker has been identified to be effective targets for CAFs. Furthermore, CAFs could be divided into different subtypes, and some subtypes may even have opposite function.[12–14] Thus, it is important to identify the molecules that are specifically expressed in CAFs, elucidate their function in tumor progression and examine whether they could be used as targets for the development of novel CAFs-targeting therapeutic strategies.

Endosialin, also known as tumor endothelial marker 1 (TEM1) or CD248, is a type I transmembrane glycoprotein that contains a C-type lectin-like domain.[15] In epithelial cell-derived cancer, endosialin was mainly expressed in tumor stroma, especially CAFs and pericytes while in mesenchymal cell-derived cancer, for example, most sarcomas, endosialin was also expressed in tumor cells, but it was rarely expressed in normal tissues.[16–19] Endosialin could promote tumor progression through different mechanisms, such as promoting tumor cell proliferation, adhesion and migration, stimulating tumor angiogenesis and inducing an immunosuppressive TME.[20] In HCC, our previous study has shown that endosialin was mainly expressed in CAFs and it could recruit and induce the M2 polarization of macrophages through the interaction with CD68 and regulation of GAS6 expression in CAFs, thus promoting HCC progression.[21] However, whether it may regulate other types of immune cells to influence TME in HCC is not known.

In this study, we found that the growth of both subcutaneous and orthotopic HCC tumors was inhibited in endosialin knockout (EN^{KO}) mice. By using single-cell RNA sequencing (scRNA-seq) analysis, mixed tumor model of HCC cells and fibroblasts, co-culture assay, chemokine array and antibody blocking assay, we showed that endosialin could inhibit the expression and secretion of CXCL9/10 in CAFs, suppress the infiltration of $CD8^+$ T cells, thus promoting HCC progression. In addition, endosialin antibody could inhibit tumor growth in vivo, and combined treatment with endosialin antibody and PD-1 antibody had synergistic antitumor effect, which may help to overcome the resistance to PD-1 blockade.

MATERIALS AND METHODS

Cell lines and isolation of primary fibroblasts

Human fibroblast HFL-1, mouse fibroblast NIH-3T3, human HSC LX-2 were purchased from the Chinese Academy of Sciences (Shanghai, China). Mouse hepatoma cell Hepa1-6 was purchased from the American Type Culture Collection (Manassas, Virginia, USA). Cells were maintained in RPMI1640 or DMEM supplemented with 10% FBS (Gibco) and 1% penicillin-streptomycin (Gibco, #15070063).

Primary CAFs and normal fibroblasts (NFs) were isolated from four HCC tumor tissues and paired adjacent normal tissues, obtained from Xijing Hospital, Fourth Military Medical University (Xi'an, China) between June and July 2023, according to previously described protocol.[22] Sequences of siRNAs or shRNAs targeting endosialin are listed in online supplemental table S1.

Flow cytometry

Tumors were isolated from host mice, minced, digested with 50 U/mL collagenase I and collagenase IV (Absin, #abs47048000) in serum-free medium for 1 hour at 37°C, then filtered through a 70 µm nylon filter (BD Biosciences) to obtain single cell suspension. After red blood cells were lysed, the remaining cells were washed twice with cold PBS. Before flow cytometry analysis, cell labeling was performed in darkness for 30 min at 4°C by incubating 1 million cells with fluorescently labeled anti-CD4 (Biolegend, #100412), anti-CD8 (Biolegend, #100708), anti-CD11b (Biolegend, #101212), anti-F4/80 (Biolegend, #123108), anti-CD86 (Biolegend, #105030), anti-CD206 (Biolegend, #141706), anti-Gr-1 (Biolegend, #108408), anti-Ly6G (Biolegend, #127606) or anti-Ly6C (Biolegend, #128014) antibodies as indicated and washed and resuspended.

Immunohistochemistry and immunofluorescent staining

Tissues from patients or mice were fixed in formalin, dehydrated in ethanol, embedded with paraffin. For clinical sample, five pairs of tumor and adjacent normal tissue specimens from five HCC patients were used for immunohistochemistry (IHC) staining, and four other tumor tissue specimens from four HCC patients were used for dual IF staining. Primary antibodies used for IHC or IF staining were anti-human endosialin (Abcam, #ab204914), anti-Ki67 (Servicebio, #GB111141-100), anti-cleaved caspase-3 (Servicebio, #GB11532-100), anti-α-SMA (Proteintech, # 14395-1-AP), anti-human CD8 (CST, #70306S), anti-mouse CD8 (CST, # 98941T) and anti-STAT1 (Proteintech, #10144-2-AP).

For IHC staining, slides were blocked with endogenous peroxidase, then incubated with goat serum for 30 min at room temperature, followed by incubation with anti-Ki67 (1:500), anti-cleaved caspase-3 (1:500), anti-human endosialin (1:1500) or anti-human CD8 (1:200) for overnight at 4°C, and immunodetection was performed on the following day using 3,3'-diaminobenzidine (DAB) according to the manufacturer's protocol. For IF staining, tumor sections were deparaffinized, rehydrated and probed with anti-human CD8 (1:100), anti-mouse CD8 (1:100), anti-α-SMA (1:800), anti-human endosialin (1:1000) antibodies. All sections were counterstained with DAPI.

For the IF staining of cells, cells cultured on cover slips were fixed with 4% paraformaldehyde for 15 min at room temperature and permeabilized with 0.2% Triton X-100 in PBS for 10 min. Cells were then blocked with goat serum for 1 hour at room temperature and then incubated with anti-STAT1 (1:50) antibody for overnight at 4°C. Cells were then incubated with Alexa Fluor-conjugated secondary antibodies (CST, #4412S) for 1 hour at room temperature. DAPI was used for counterstaining of nuclei, and images were captured using laser scanning confocal microscopy.

Western blot

Cells with downregulated or overexpressed endosialin and their control cells were cultured in DMEM with 10% serum until 90% confluency. Cells were then cultured in fresh serum-free medium containing 20 ng/mL IFN-γ (Sino Biological, #11725-HNAE) for 24 hours, before they were lysed in ice-cold RIPA buffer. Total protein was quantified using BCA method according to manufacturer's protocol before Western blot (WB) analysis. Briefly, 8% SDS-PAGE were equi-loaded with 20–30 µg protein, electrophoresed at 100 V and electro-transferred to nitrocellulose membranes. After blocking with 5% BSA, membranes were incubated with primary antibodies for overnight at 4°C, followed by incubation with horseradish peroxidase-conjugated secondary antibodies and then visualized by chemiluminescence. The primary antibodies used in WB were: anti-human endosialin (Abcam, #ab204914), anti-mouse endosialin (Santa, #sc-377221), anti-STAT1 (Proteintech, #10144-2-AP), anti-P-STAT1 (Proteintech, #80115-1-RR), anti-GAPDH (Proteintech, #10494-1-AP), anti-α-SMA (Proteintech, #14395-1-AP).

Reverse transcription-qPCR

Total RNA was isolated with Trizol, and reverse transcription (RT) was performed using PrimeScript RT Master Mix (TaKaRa). Then, qPCR was performed using a SYBR Green II Kit (TaKaRa, #DRR041A). Primers used for qPCR are summarized in online supplemental table S2.

In vitro co-culture assay

Fibroblasts with downregulated or overexpressed endosialin and their control cells (7×10^4) were seeded in 24-well plates and cultured for 24 hours. Meanwhile, human peripheral blood mononuclear cells were isolated from healthy donors, and T cells were isolated using Dynabeads FlowComp human CD3 kit (#11365D, Invitrogen). T cells were labeled with 5(6)-carboxyfluorescein diacetate N-succinimidyl ester (CFSE) and seeded in 3 µm chambers (5×10^5) containing serum-free 1640 medium. The chambers were then placed in the 24-well plates which contained 10% serum 1640 medium and were seeded with fibroblasts (6×10^4) and co-cultured for 24 hours. After co-culture, chambers were taken out, fixed with paraformaldehyde, wiped off the upper chamber cells with a cotton swab, and washed three times with PBS. Migrated cells were counted under a fluorescence microscopy using a magnification of 20×for quantifying images. For antibody blocking experiments, CXCL10 neutralizing antibody or control antibody (RD, #MAB266-SP) were added to the lower chamber of the transwell, and after co-culture for 24 hours, the chamber was removed and migrated T cells were counted as mentioned above.

RNA-seq

Total RNAs were extracted from tumor tissues of EN^{KO} or WT mice with Trizol (Invitrogen). The quality of RNA was checked by Bioanalyzer 2200 (Aligent) and kept at −80°C. The RNA with RIN>6.0 was qualified for experiment. The tagged cDNA libraries were pooled in equal ratio and used for 150 bp paired-end sequencing in a single lane of the Illumina HiSeq×Ten. HTseq was used to count gene and lncRNA counts and RPKM method was used to determine gene expression.[23]

To explore the function of endosialin in HCC TME, we performed Gene Ontology (GO) terms and Kyoto Encyclopedia of Genes and Genomes (KEGG) pathway enrichment analysis using "cluster Profiler (4.4.4)", "GO plot (1.0.2)", "ggplot2" and their dependency packages in R (V.4.2.1). Fisher's exact test was applied to identify the significant GO categories and FDR was used to correct the p values.

Single-cell RNA Sequencing

Tumor tissues from EN^{KO} and WT mice were isolated and kept in MACS Tissue Storage Solution (Miltenyi Biotec) until processing. Tumor tissues were processed as described below. Briefly, samples were first washed with PBS, minced into small pieces (approximately 1 mm^3) on ice and enzymatically digested with 150 U/mL collagenase II (Worthington) and 2 mg/mL collagenase IV (Worthington) and 1.2 U/mL Dispase II (Worthington) and 50 U/mL DNase I for 50 min at 37 °C, with agitation. After digestion, samples were sieved through a 70 µm cell strainer, and centrifuged at 300 g for 5 min. After the supernatant was removed, the pelleted cells were suspended in red blood cell lysis buffer (Miltenyi Biotec) to lyse red blood cells. After washing with PBS containing 0.04% BSA, the cell pellets were resuspended in PBS containing 0.04% BSA and refiltered through a 35 µm cell strainer. Dissociated single cells were then stained with AO/PI for viability assessment using Countstar Fluorescence Cell Analyzer.

ScRNA-Seq libraries were generated using 10×Genomics Chromium Controller Instrument and Chromium Single Cell 3' V3 Reagent Kits (10×Genomics, Pleasanton, Califonia, USA). ScRNA-seq data analysis was performed by NovelBio with NovelBrain Cloud Analysis Platform (www.novelbrain.com). Seurat package (V.3.1.4, https://satijalab.org/seurat/) was used for cell normalization and regression based on the expression table according to the UMI counts of each sample and percentage of mitochondria rate to obtain scaled data. PCA was constructed based on the scaled data with top 2000 high variable genes and top 10 principles were used for T-Distributed

Stochastic Neighbor Embedding (tSNE) construction and Uniform Manifold Approximation and Projection (UMAP) construction. Using graph-based cluster method, we acquired the unsupervised cell cluster result based on the PCA top 10 principal and we calculated the marker genes by FindAllMarkers function with Wilcoxon rank sum test algorithm under following criteria: (1) log2FC>0.25; (2) <0.05; and (3) min.pct>0.1. In order to identify the detailed cell type, the clusters of same cell type were selected for re-tSNE analysis, graph-based clustering and marker analysis.

To identify differentially expressed genes (DEGs) among samples, the function FindMarkers with Wilcoxon rank sum test algorithm was used under following criteria: (1) InFC>0.25; (2) p<0.05; and (3) min.pct>0.1.

Establishment and treatment of mouse HCC tumor models

Animal experiments in this study were approved by the Laboratory Animal Welfare and Ethics Committee of the Northwestern Polytechnical University. EN^{KO} C57BL/6 mice were purchased from the Shanghai Model Organisms Center (Shanghai, China; #NM-KO-200094). The EN^{KO} mice were whole-body knockout and were generated by using CRISPR/Cas9 technology to delete the exon 1 of endosialin and introduce frameshift mutations through non-homologous recombination repair mechanism. Wild-type (WT) C57BL/6 mice were purchased from the Animal Center of the Fourth Military Medical University (Xi'an, China) and kept at the same feeding level as EN^{KO} mice for 1–2 weeks before experiments. Mouse hepatoma cell Hepa1-6 was used to establish subcutaneous or orthotopic HCC tumor models. For subcutaneous tumor, 5×10^6 Hepa1-6 cells were inoculated into each EN^{KO} or WT mouse (4–6 weeks, male, body weight 20–30 g). For orthotopic tumor, Hepa1-6 cells expressing luciferase were mixed with Matrigel at a 1:1 ratio and injected into the liver after it was fully exposed by surgery, according to the protocol that was described in detail previously.[24] For mixed tumor model, a mixture of 5×10^6 Hepa1-6 cells and 1.5×10^7 NIH-3T3 cells that had been infected with lentiviruses expressing shEN or shCtrl was inoculated into each WT C57BL/6 mouse (4–6 weeks, male, body weight 20–30 g).

For antibody treatment, mice were treated with anti-mouse PD-1 antibody (5 mg/kg; Bio×Cell) with or without endosialin antibody (5 mg/kg) from day 8 after inoculation, every 3 days for a total of four times. Tumor size was measured every 3 days and tumor growth curves were drawn. At the end of the experiment, mice were sacrificed, and tumors were isolated for subsequent experiments.

Chemokine array

A human chemokine array kit (RD, #ARY017) was used according to the manufacturer's protocol. Briefly, the membranes were blocked at room temperature for 1 hour, and 500 µL of siEN or siCtrl cell culture medium was mixed with Detection Antibody Cocktail and incubated for 1 hour, and then sample/antibody mixtures were added to the two membranes, respectively, and incubate overnight at 4°C. Membranes were washed twice, and Streptavidin-HRP was added to each membrane and incubated for 30 min at room temperature. Carefully wash the membrane twice and incubate the membrane with a chemiluminescent substrate followed by image visualization.

ELISA

Cells with downregulated or overexpressed endosialin and their control cells were cultured in DMEM with 10% serum until 90% confluency. Cells were then cultured in fresh serum-free media containing 20 ng/mL IFN-γ. The supernatants of cells were harvested 24 hours later, and human CXCL9 (CUSABIO, #CSB-E09024h) and CXCL10 (CUSABIO, #CSB-E08181h) ELISA kits were used to examine their levels. Experiment was performed according to the manufacturer's instructions.

To examine CXCL9/10 level in the tumor tissues of EN^{KO} or WT mice, tumor tissues were isolated and prepared into a tissue homogenate by tissue fragmentation, and then examined using mouse CXCL9 (CUSABIO, #CSB-EL006252MO) and CXCL10 (CUSABIO, #CSB-E08183m) ELISA kits according to the manufacturer's instructions.

Statistical analysis

All statistical analyses were performed by using IBM SPSS statistical (V.23) or GraphPad Prism V.8 software. Quantitative data were subjected to a normality test and an equality test of variances before analysis. Data were presented as mean±SD or mean±SEM. Comparisons were analyzed using two-tailed Student's t-test or one-way analysis of variance followed by Dunnett's post hoc test. Differences were considered statistically significant at p<0.05.

RESULTS

Tumor growth of HCC is inhibited in endosialin knockout mice

To study the function of endosialin in HCC, we established subcutaneous HCC tumor model by inoculating Hepa1-6 cells into endosialin knockout (EN^{KO}) mice (online supplemental figure 1A,B) and WT mice and observed the tumor growth. Results showed that compared with WT mice, tumor growth was significantly inhibited in EN^{KO} mice (figure 1A,B). Immunohistochemical staining of Ki67 and cleaved caspase-3 revealed that tumor cell proliferation was inhibited while apoptosis was increased in the tumor tissues of EN^{KO} mice (figure 1C). We also generated orthotopic HCC tumor model by injecting luciferase-expressing Hepa1-6 cells into the livers of EN^{KO} mice and WT mice and found that growth of orthotopic tumors was also inhibited in EN^{KO} mice, as shown by the decreased fluorescence signal through in vivo imaging (figure 1D,E).

HCC tissues from endosialin knockout mice have increased $CD8^+$ T cell infiltration

To clarify how endosialin affects HCC progression, we performed scRNA-seq analysis using freshly isolated subcutaneous tumors from EN^{KO} mice and WT mice

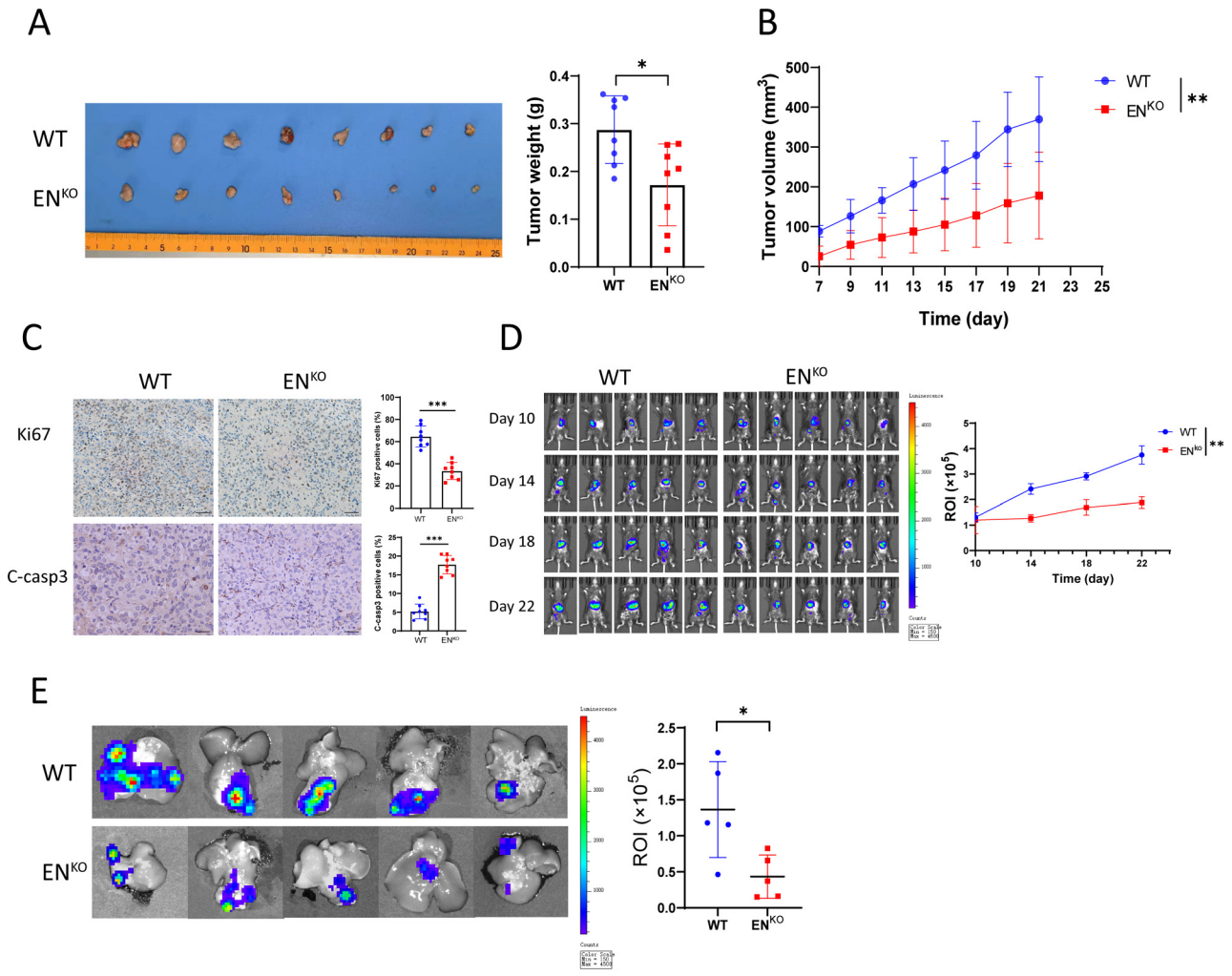

Figure 1 Tumor growth of hepatocellular carcinoma (HCC) is inhibited in endosialin knockout mice. (A) Subcutaneous Hepa1-6 tumors from wild type (WT) and endosialin knockout (EN^{KO}) mice (left) and the tumor weight (right) at day 21 after mice were sacrificed. (B) Growth curve of the tumors in WT and EN^{KO} mice. (C) Immunohistochemistry (IHC) staining of Ki67 and cleaved caspase-3 in the tumor tissues from WT and EN^{KO} mice. Scale bar, 50 µm. (D) Bioluminescence imaging (BLI) (left) and standardized region of interest (ROI) (right) to show the growth of orthotopic Hepa1-6-Luc tumors in WT and EN^{KO} mice. (E) BLI (left) and standardized ROI (right) to show the growth of orthotopic Hepa1-6-Luc tumors in isolated liver tissues from WT and EN^{KO} mice. Data are presented as the mean±SEM. *p<0.05; **p<0.01.

(figure 2A, online supplemental figure 2A). Results showed that the number of infiltrated CD8$^+$ T cells was significantly higher in EN^{KO} mice than WT mice, and it seemed that the infiltrated CD8$^+$ T cells were more activated, as shown by the increased level of Cd69 and Ifn-γ (figure 2B, online supplemental figure 2B). We also examined the infiltration of CD8$^+$ and CD4$^+$ T cells in the tumor tissues of EN^{KO} and WT mice by flow cytometry, and results confirmed that tumor tissues from EN^{KO} mice had significantly higher CD8$^+$ T cell infiltration than those from WT mice, while the infiltration of CD4$^+$ T cell did not show a significant difference (figure 2C). We also performed IF and IHC staining of CD8 on the sections of orthotopic tumors from EN^{KO} and WT mice and found that in WT mice, most CD8$^+$ T cells were located at the tumor margin area while in EN^{KO} mice, a lot more CD8$^+$ T cells existed in the central area of tumors (figure 2D,E). These data indicate that endosialin may suppress the infiltration of CD8$^+$ T cells into tumor tissues.

We also examined whether loss of endosialin may have effects on other types of immune cells in the TME of subcutaneous tumors by flow cytometry. Results showed that, compared with WT mice, the total number of macrophages did not show significant difference, however, the number of M2 macrophages decreased while M1 macrophages increased in EN^{KO} mice (online supplemental figure 2C,D). We also examined the number of myeloid-derived suppressor cells (MDSCs) and found that total MDSCs, granulocyte-like MDSCs (G-MDSCs) and monocytes-like MDSCs (M-MDSCs) were all decreased in EN^{KO} mice than WT mice (online supplemental figure 2E–G). These results indicate that endosialin plays an important role in the formation of immunosuppressive TME.

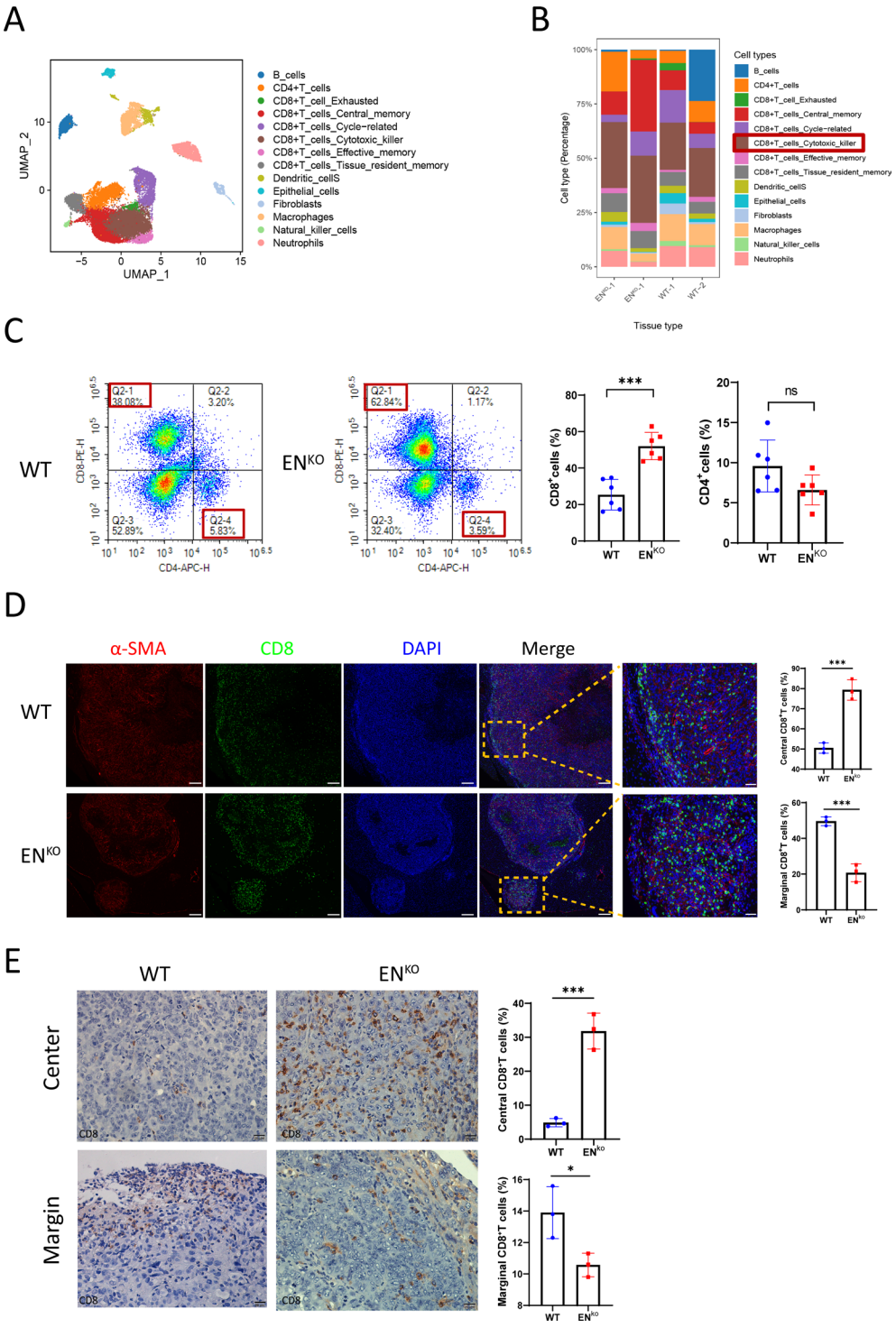

Figure 2 Hepatocellular carcinoma (HCC) tissues from endosialin knockout mice have increased CD8$^+$ T cell infiltration. (A) UMAP visualization of the cell populations in subcutaneous Hepa1-6 tumor tissues from wild type (WT) and endosialin knockout (EN^{KO}) mice. (B) Bar plots to show the proportion of different cell types in the tumor tissues from WT and EN^{KO} mice. (C) Flow cytometry to show the percentage of CD4$^+$ T cells and CD8$^+$ T cells in the tumor tissues from WT and EN^{KO} mice (left) and quantification of the flow cytometry data (right) (n=6). (D) Dual immunofluorescent (IF) staining of α-SMA and CD8 in orthotopic Hepa1-6 tumor tissues from WT and EN^{KO} mice. Scale bar, 100 µm (left) and 20 µm (rightmost). (E) Immunohistochemistry (IHC) staining of CD8 in the center (top) and margin (bottom) of orthotopic Hepa1-6 tumor tissues from WT and EN^{KO} mice. Scale bar, 20 µm. Representative images are shown. Data are presented as the mean±SEM. *p<0.05; ***p<0.001; ns, not significant. UMAP, Uniform Manifold Approximation and Projection.

Endosialin-positive CAFs promote tumor growth by suppressing CD8+ T infiltration

To further clarify the function of endosialin-positive CAFs in HCC progression, we established mixed tumor model through subcutaneously injecting Hepa1-6 cells and endosialin knockdown or control NIH-3T3 cells into C57BL/6 mice. The knockdown efficiency of endosialin in NIH-3T3 cells was confirmed by RT-qPCR and WB (online supplemental figure 3A,B). The growth of tumors was monitored and results showed that the existence of NIH-3T3 cells could promote tumor growth, however, when endosialin was knocked down, their tumor-promoting effect was obviously diminished (figure 3A,B). By using flow cytometry analysis, we analyzed the infiltration of $CD8^+$ and $CD4^+$ T cells in the mixed tumor tissues and found that knockdown of endosialin in NIH-3T3 cells significantly promoted the infiltration of $CD8^+$ T cells while the infiltration of $CD4^+$ T cells was not influenced (figure 3C). In addition, we also found that knockdown of endosialin in NIH-3T3 cells also could significantly inhibit the recruitment of MDSCs (online supplemental figure 3C).

To examine whether endosialin-positive fibroblasts may influence $CD8^+$ T cell migration in vitro, we performed co-culture assay using endosialin knockdown or control NIH-3T3 cells, and CFSE labeled mouse T cell line CTLL2 in transwell chambers. Results showed that knockdown of endosialin in NIH-3T3 cells significantly promoted the migration of CTLL2 cells (figure 3D). We also performed co-culture assay using endosialin knockdown or control human fibroblast HFL1 cells and freshly isolated human T cells and obtained similar results (figure 3E). Furthermore, we overexpressed endosialin in human HSC LX-2 cells and co-cultured them with human T cells and found that the overexpression of endosialin in LX-2 cells could significantly inhibit the migration of T cells (figure 3F). Based on these results, we speculate that endosialin-positive CAFs may promote tumor growth by suppressing $CD8^+$ T infiltration.

Knockdown of endosialin promotes the expression and secretion of CXCL9/10 in CAFs by activating IFN-γ-STAT1 pathway

To clarify the mechanism how endosialin-positive CAFs inhibit $CD8^+$ T cell infiltration, we first analyzed the potential correlation between endosialin and immune cell migration in HCC in TCGA database. GO and KEGG enrichment analysis showed that endosialin was associated with lymphocyte migration, cell chemotaxis, and chemokine signaling pathway (online supplemental figure 4A,B). To examine whether endosialin may influence the expression and secretion of certain chemokines in CAFs, we collected the culture medium from IFN-γ stimulated endosialin knockdown or control HFL1 cells and performed chemokine array assay. Results showed that compared with control cells, the levels of CXCL9 and CXCL10, which play important role in $CD8^+$ T cell infiltration, were significantly increased in the culture medium of endosialin knockdown HFL1 cells (figure 4A). The increased expression and secretion of CXCL9/10 in endosialin knockdown HFL1 cells were also validated by RT-qPCR and ELISA (figure 4B,C). We also examined the expression and secretion of CXCL9/10 in endosialin overexpressing LX-2 cells and obtained consistent results, as shown by the obviously decreased mRNA and protein level of CXCL9/10 in endosialin overexpressing LX-2 cells (figure 4D,E). In addition, we also examined the level of CXCL9/10 in the tumor tissues of EN^{KO} and WT mice by ELISA and found that the level of CXCL9/10 was much higher in the tumor tissues of EN^{KO} mice than that of WT mice (figure 4F). Next, we examined whether the increased T cell migration by endosialin knockdown fibroblasts is dependent on CXCL10 through co-culture assay of HFL1 cells and T cells in the presence of CXCL10 neutralizing antibody and found that when CXCL10 neutralizing antibody was added, the increased T cell migration was inhibited again (figure 4G).

Then, to explore the mechanism how endosialin regulates CXCL9/10 expression, we performed RNA-Seq using the RNA isolated from tumor tissues of EN^{KO} and WT mice, and results showed that CXCL9/10 were among the upregulated chemokines in tumors of EN^{KO} mice than those of WT mice (online supplemental figure 4C). GO analysis of the DEGs in tumor tissues of EN^{KO} and WT mice showed that endosialin expression was significantly correlated with the genes that regulate T cell migration and cell chemotaxis (online supplemental figure 4D). KEGG enrichment analysis showed that DEGs were enriched in JAK/STAT signaling pathway, which has been reported to regulate CXCL9/10 expression and secretion under IFN-γ stimulation[25–27] (online supplemental figure 4E).

So, we examined whether endosialin could influence the activation of INF-γ-STAT1 pathway in HFL1 cells, results showed that in endosialin knockdown cells, after IFN-γ stimulation, both the phosphorylation and nuclear translocation of STAT1 were significantly increased than control cells (figure 4H,I). We also examined whether overexpression of endosialin may influence the activation of INF-γ-STAT1 pathway, and results showed that both phosphorylation and nuclear translocation of STAT1 were obviously inhibited in endosialin overexpressing LX-2 cells (figure 4J,K). These results demonstrate that endosialin inhibits CXCL9/10 expression and secretion in CAFs by inhibiting INF-γ-STAT1 signaling pathway.

High endosialin expression is correlated with low $CD8^+$ T infiltration in clinical HCC tissues

To confirm our findings in clinical samples, we first examined the expression of endosialin by IHC in HCC tissues and adjacent normal tissues and found that endosialin expression was significantly higher in HCC tissues than adjacent normal tissues (figure 5A, online supplemental figure 5A). We also isolated CAFs from tumor tissues and NFs from adjacent normal tissues of HCC patients, and examined the level of endosialin by RT-qPCR and

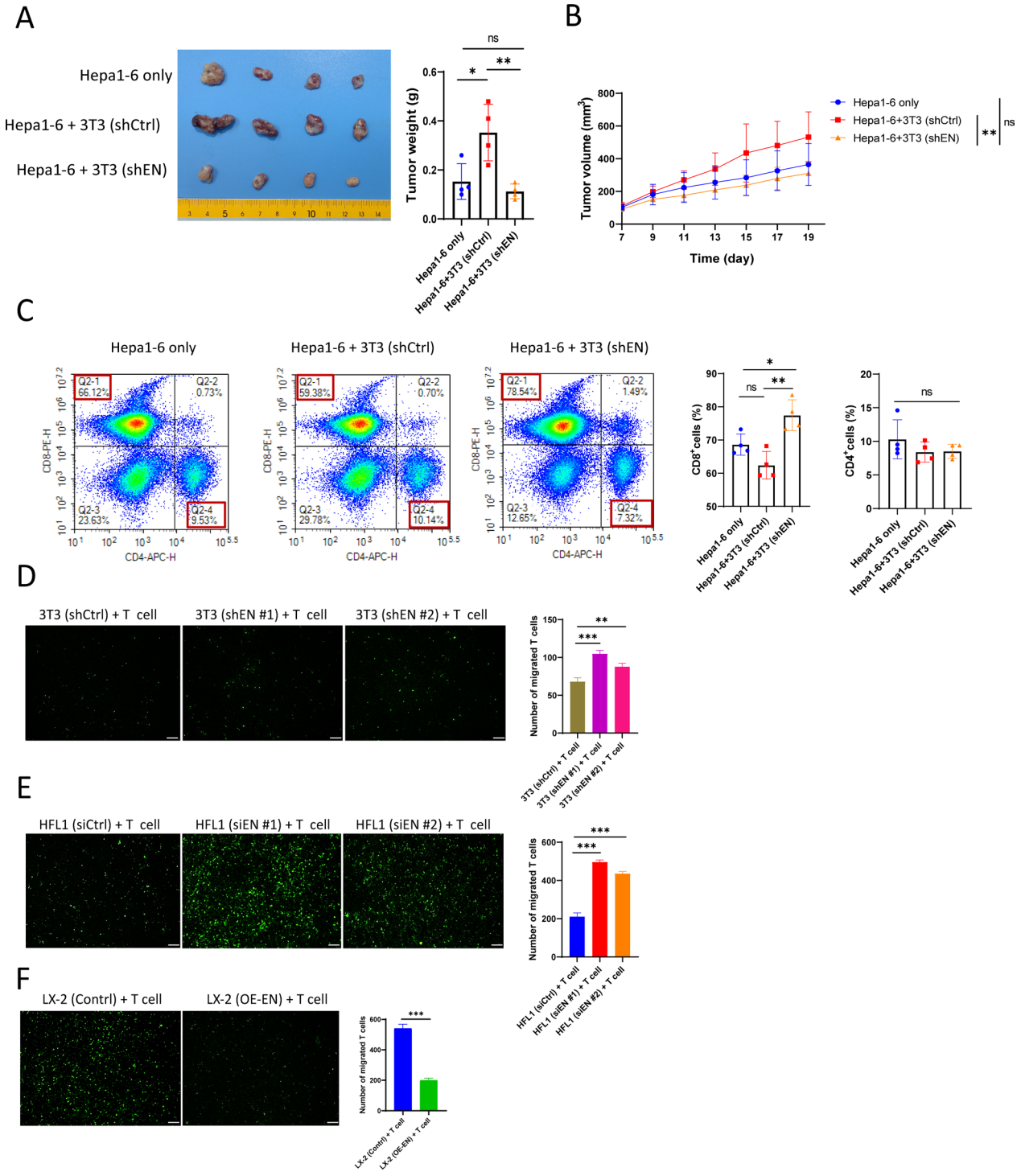

Figure 3 Endosialin-positive cancer-associated fibroblasts (CAFs) promote tumor growth by suppressing CD8⁺ T infiltration. (A) Picture of the tumors with mixed Hepa1-6 cells and endosialin knockdown or control NIH-3T3 cells (left) and the tumor weight (right) at day 19 after mice were sacrificed (n=4). (B) Growth curve of the indicated tumors. (C) Flow cytometry to show the percentage of CD4⁺ T cells and CD8⁺ T cells in indicated tumor tissues (left panel) and quantification of the flow cytometry data (right panel) (n=4). (D–F) Fluorescent imaging to show the migrated 5(6)-carboxyfluorescein diacetate N-succinimidyl ester (CFSE)-labeled mouse or human T cells after co-culture with endosialin knockdown or control NIH-3T3 cells (D) or HFL1 cells (E), or endosialin overexpressing or control LX-2 cells (F) (left panel) and quantification of the migrated T cells (right). Scale bar, 100 µm. Representative images are shown. Data are presented as the mean±SEM. *p<0.05; **p<0.01; ***p<0.001; ns, not significant.

WB, results confirmed that endosialin expression was much higher in CAFs from different patients than NFs (online supplemental figure 5C,D). Then we examined the correlation between endosialin expression and CD8⁺ T cell infiltration by dual IF staining and found that the regions with high endosialin expression (EN^{high}) had

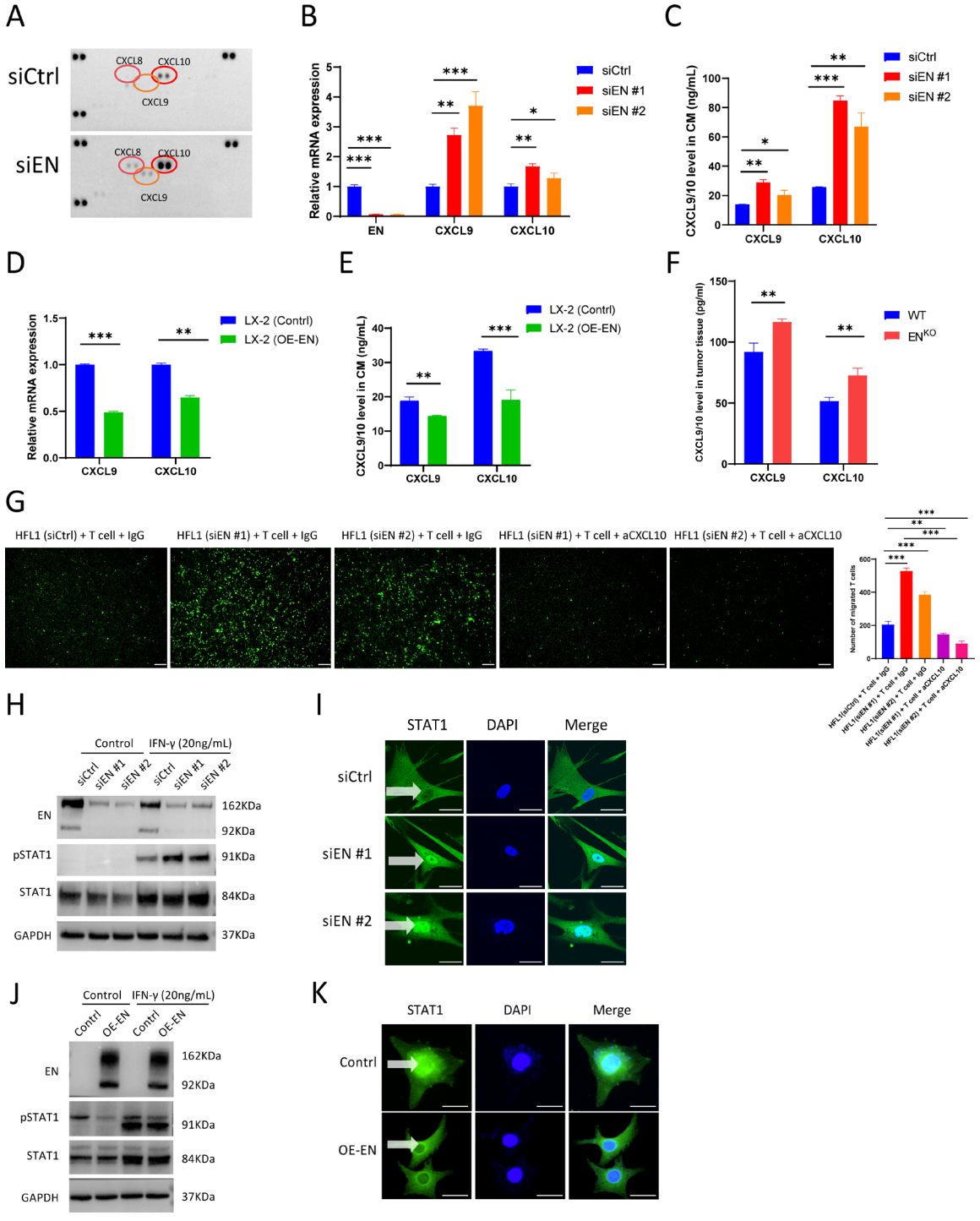

Figure 4 Knockdown of endosialin promotes the expression and secretion of CXCL9/10 in cancer-associated fibroblasts (CAFs) by activating INF-γ-STAT1 pathway. (A) Chemokine array to show the levels of different chemokines in IFN-γ-stimulated endosialin knockdown or control HFL1 cells. (B) RT-qPCR to show the mRNA level of CXCL9/10 in endosialin knockdown or control HFL1 cells. (C) ELISA to show the protein level of CXCL9/10 in the culture medium of endosialin knockdown or control HFL1 cells. (D) RT-qPCR to show the mRNA level of CXCL9/10 in endosialin overexpressing or control LX-2 cells. (E) ELISA to show the protein level of CXCL9/10 in the culture medium of endosialin overexpressing or control LX-2 cells. (F) ELISA to show the level of CXCL9/10 in subcutaneous Hepa1-6 tumor tissues of WT and EN^{KO} mice (n=3). (G) Fluorescent imaging to show the migrated 5(6)-Carboxyfluorescein diacetate N-succinimidyl ester (CFSE)-labeled T cells after co-culture with endosialin knockdown or control HFL1 cells in the presence of CXCL10 neutralizing antibody or control antibody (left) and quantification of the migrated T cells (right). Scale bar, 100 µm. (H) Western blot to detect the level of pSTAT1 in endosialin knockdown or control HFL1 cells. (I) IF staining to show the localization of STAT1 in endosialin knockdown or control HFL1 cells. Scale bar, 20 µm. (J) Western blot to detect the level of pSTAT1 in endosialin overexpressing or control LX-2 cells. (K) IF staining to show the localization of STAT1 in endosialin overexpressing or control LX-2 cells. Scale bar, 20 µm. Representative images are shown. Data are presented as the mean±SEM. *p<0.05; **p<0.01; ***p<0.001.

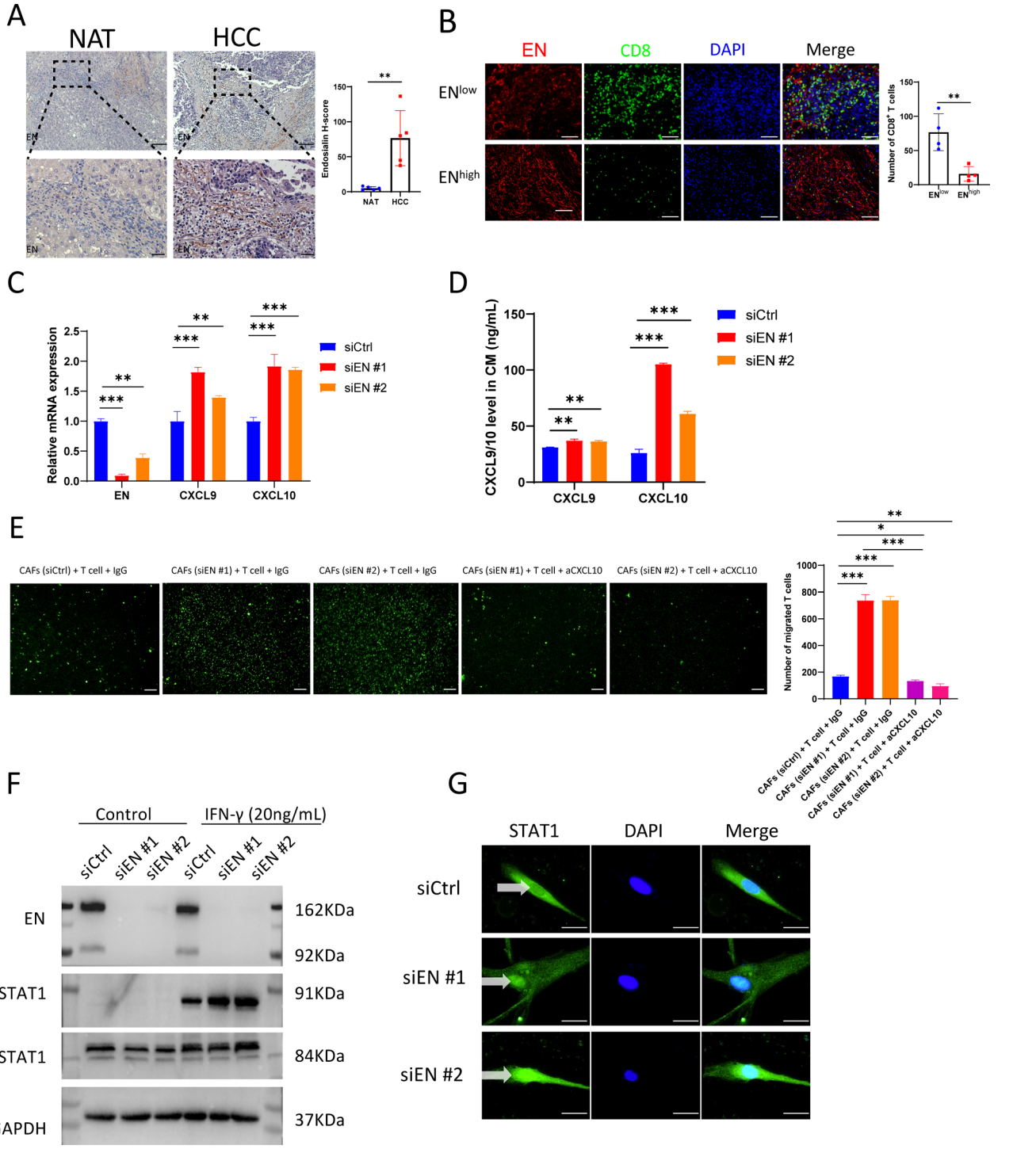

Figure 5 High endosialin expression is correlated with low CD8$^+$ T infiltration in clinical hepatocellular carcinoma (HCC) tissues. (A) Immunohistochemistry (IHC) staining of endosialin in HCC tissues and adjacent normal tissues (n=5). Scale bar, 100 µm (top panel), 20 µm (bottom panel). (B) Dual immunofluorescent (IF) staining of HCC tissues to show the correlation between endosialin expression and CD8$^+$ T cell infiltration (n=4). Scale bar, 50 µm. (C) RT-qPCR to show the mRNA level of CXCL9/10 in endosialin knockdown or control primary cancer-associated fibroblasts (CAFs. (D) ELISA to show the protein level of CXCL9/10 in the culture medium of endosialin knockdown or control primary CAFs. (E) Fluorescent imaging to show the migrated 5(6)-carboxyfluorescein diacetate N-succinimidyl ester (CFSE)-labeled T cells after co-culture with endosialin knockdown or control primary CAFs at the presence of CXCL10 neutralizing antibody or control antibody (left) and quantification of the migrated T cells (right). Scale bar, 100 µm. (F) Western blot to detect the level of pSTAT1 in endosialin knockdown or control primary CAFs. (G) IF staining to show the localization of STAT1 in endosialin knockdown or control primary CAFs. Scale bar, 20 µm. Representative images are shown. Data are presented as the mean±SEM. *p<0.05; **p<0.01; ***p<0.001.

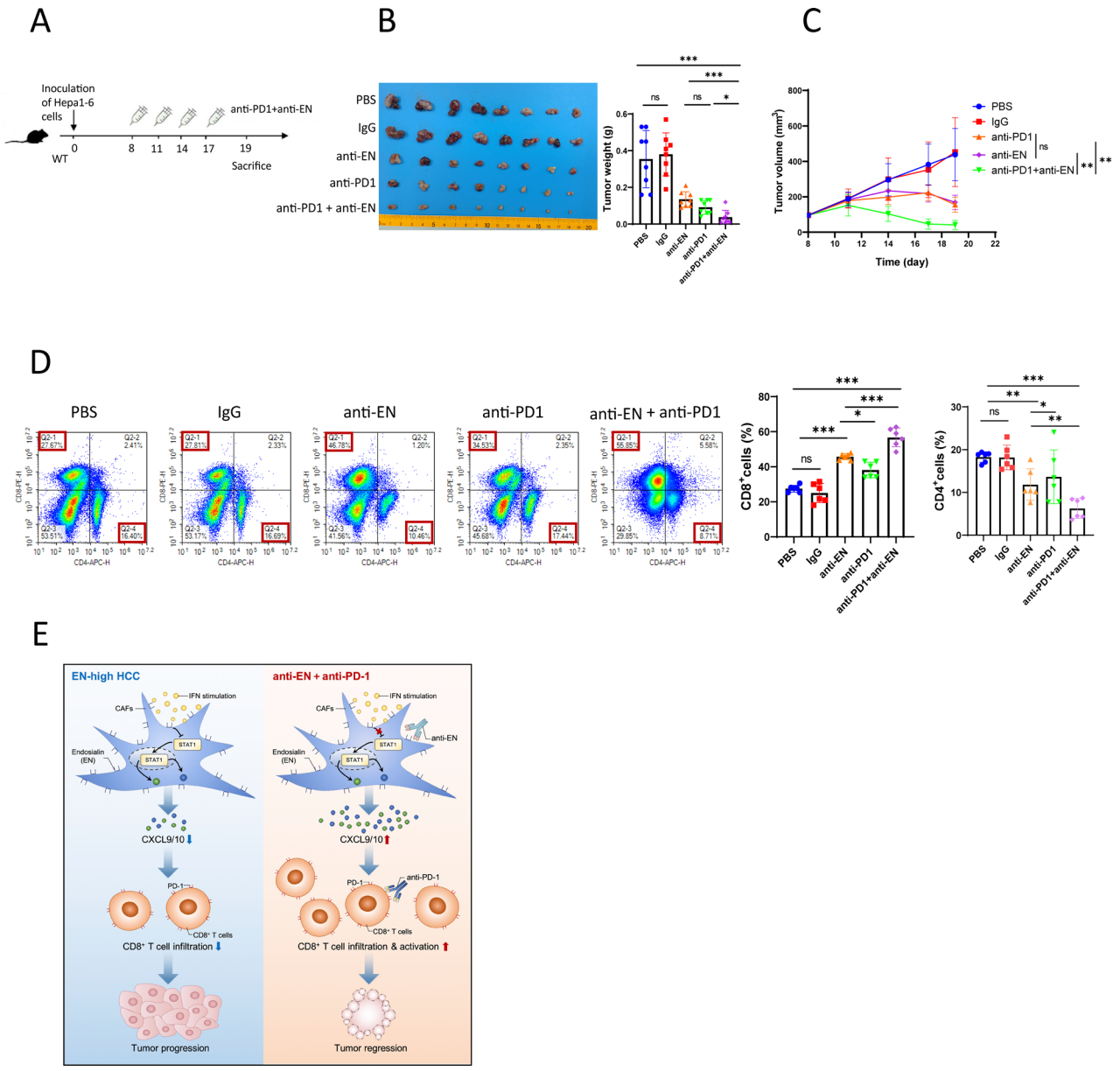

Figure 6 Combination therapy with endosialin antibody and PD-1 antibody shows synergistic antitumor effect. (A) Schematic image to show the process of combination therapy. (B) Picture of isolated tumors (left) and tumor weight (right) after mice were sacrificed after treatment (n=8). (C) Growth curve of the tumors in different groups after treatment. (D) Flow cytometry to show the percentage of $CD4^+$ T cells and $CD8^+$ T cells in the tumor tissues of different groups after treatment (left panel) and quantification of the flow cytometry data (right panel) (n=6). (E) Graphic diagram to describe the function of endosialin, which can inhibit the secretion of CXCL9/10 by inhibiting IFN-γ/JAK/STAT1 pathway in CAFs, thus inhibit the infiltration of $CD8^+$ T cells into tumor tissues; and endosialin antibody can enhance the anti-tumor effect of PD1 antibody by increasing the infiltration of $CD8^+$ T cells. Representative images are shown. Data are presented as the mean±SEM. *p<0.05; **p<0.01; ***p<0.001; ns, not significant. CAFs, cancer-associated fibroblasts.

low $CD8^+$ T cell infiltration while regions with low endosialin expression (EN^{low}) had obviously higher $CD8^+$ T cell infiltration (figure 5B, online supplemental figure 5B). To further confirm whether endosialin could inhibit CXCL9/10 expression and secretion in primary CAFs, we also knocked down endosialin in primary CAFs and examined the expression and secretion level of CXCL9/10 by RT-qPCR and ELISA and confirmed that knockdown of endosialin also could upregulate CXCL9/10 expression and secretion in primary CAFs (figure 5C,D). Furthermore, the existence of CXCL10 neutralizing antibody also inhibited the increased T cell migration induced by endosialin knockdown primary CAFs in co-culture assay (figure 5E). In addition, the phosphorylation and nuclear translocation of STAT1 were also increased in endosialin knockdown primary CAFs under IFN-γ stimulation (figure 5F,G).

Combination therapy with endosialin antibody and PD-1 antibody shows synergistic antitumor effect

Based on the findings that downregulation of endosialin could promote CD8$^+$ T cell migration, we speculate that combination therapy with endosialin antibody and PD-1 antibody may have synergistic antitumor effect. So, we treated tumor-bearing C57BL/6 mice with endosialin antibody Ig78 and mouse PD-1 antibody and found that combined treatment had obviously enhanced antitumor effect than either antibody alone (figure 6A–C). After treatment, we examined the T cell infiltration in tumor tissues by flow cytometry and found that CD8$^+$ T cell infiltration was increased in the tumors treated with either antibody alone, however, combined treatment had a lot more CD8$^+$ T cell infiltration than either single antibody group. Interestingly, CD4$^+$ T cell infiltration was inhibited in the tumors treated with either antibody alone, and combined treatment resulted in much lower CD4$^+$ T cell infiltration (figure 6D). We also examined the number of MDSCs in tumor tissues by flow cytometry after treatment and found that combined treatment did not show synergistic effect in MDSCs recruitment, although single antibody alone showed inhibited MDSCs recruitment (online supplemental figure 6). These data indicate endosialin antibody can inhibit tumor growth in vivo, and combination therapy with PD-1 antibody has synergistic antitumor effect than single antibody alone, which may overcome the resistance to PD-1 blockade (figure 6E).

DISCUSSION

CAFs are the most important components in TME and play critical role in HCC progression. The elucidation of the mechanism by which CAFs promote HCC progression will help to identify novel therapeutic targets and develop new therapeutic strategies.

Studies have found that CAFs could promote HCC progression through different mechanisms. For example, CAFs could produce type I collagen to increase the stiffness and TAZ activation in pretumoral hepatocytes and activate discoidin domain receptor 1 (DDR1) in established tumors, thus promote cell proliferation and HCC development.[28] CAFs could secrete sulfatase-2 (SULF2) to promote HCC cell proliferation, invasion, and sorafenib resistance through IKKβ/NF-κB pathway, and also increase the macrophage recruitment and phenotype alteration in TME.[29] CAFs could secrete cardiotrophin-like cytokine factor 1 (CLCF1) to induce the secretion of chemokine (C-X-C motif) ligand 6 (CXCL6) and TGF-β in tumor cells, thus to promote tumor cell stemness and TAN infiltration and polarization.[30] CAFs could also secrete macrophage migration inhibitory factor (MIF) to recruit CD33$^+$ MDSCs, thus providing an immunosuppressive TME.[31]

Because of their tumor-promoting function, CAFs have been considered as ideal targets for HCC treatment. Some CAF-targeting therapeutic strategies have been developed, however, most of them target either CAF-derived paracrine productions or CAF's downstream signaling pathway, which do not have high specificity for CAFs.[32–35] Until now, fibroblast activation protein (FAP) was the only membrane protein that was considered as an ideal surface molecule for CAF-targeting therapy. Although several studies designed different FAP-targeting vaccine or nanoparticle mediated therapeutic strategies in different cancer types, however, they have not been examined in HCC.[36–38] Yet, it is worth noting that a phase II clinical trial of FAP antibody in patients with metastatic colorectal cancer failed due to limited clinical response.[39] In addition, it has been found that FAP was also highly expressed in skeletal muscle and bone marrow, and the depletion of FAP positive stromal cells resulted in cachexia and anemia.[40] Thus, more CAF-specific membrane molecules need to be identified.

Endosialin (endosialin) is a transmembrane glycoprotein that is highly expressed in tumor stromal cells such as CAFs and pericytes, as well as in cancer cells in most sarcomas. In addition to its specific expression, studies have also found that endosialin could promote tumor progression through different mechanisms, which has been systemically reviewed by our team.[20] In HCC, our previous study has found that endosialin-positive CAFs could recruit and induce the M2 polarization of macrophages, thus promoting HCC progression.[21] However, whether they may regulate other types of immune cells to influence TME in HCC is not known.

Here, in this study, we found that the growth of both subcutaneous and orthotopic HCC tumors was significantly inhibited in EN^{KO} mice. By using scRNA-seq analysis, we found that the infiltration of CD8$^+$ T cells in the tumor tissues of EN^{KO} mice was much higher than those in WT mice. By using co-culture assay, we confirmed that knockdown of endosialin in CAFs could significantly promote T cell migration in vitro. Then, by using chemokine array, ELISA, RT-qPCR and antibody blockade assay, we demonstrated that endosialin could inhibit T cell migration by inhibiting the expression and secretion of CXCL9/10 in CAFs. At last, by using RNA-seq analysis and confirmative experiments, we demonstrated that endosialin could inhibit the activation of INF-γ-STAT1 pathway, inhibit CXCL9/10 expression and secretion, and suppress CD8$^+$ T cell infiltration, thus promoting HCC progression.

In last decade, the application of immunotherapy, especially ICI like camrelizumab, nivolumab and pembrolizumab, has opened up new treatment options for HCC.[41] Clinical studies have shown that some patients did have a complete or partial response, however, there still have pretty many patients who do not respond to ICI treatment.[42–44] Until now, several combination therapeutic strategies have also been approved by FDA for the treatment of HCC, like atezolizumab (anti-PD-L1) plus bevacizumab (anti-VEGF), and durvalumab (anti-PD-1) plus tremelimumab (anti-CTLA4).[45 46] However, certain percentage of patients still do not response to these treatments. Furthermore, no validated biomarkers have been

identified that could guide clinical decision-making.[47] It has been found that CAFs and TME could influence patients' response to ICI treatment, thus, it is important to identify the factors that are involved in CAFs function and in the formation of immunosuppressive TME.[48 49]

$CD8^+$ T cells are the most powerful effectors in antitumor immune response and play central role in the elimination of tumor cells after ICI treatment.[50 51] Since our study indicated that endosialin-positive CAFs could inhibit $CD8^+$ T cell infiltration, we speculate that the blockade of endosialin might increase the infiltration of $CD8^+$ T cells and combination therapy with endosialin antibody and PD-1 antibody may have enhanced antitumor effect. Thus, we treated the HCC tumor-bearing mice using endosialin antibody and PD-1 antibody and found that combination therapy did have synergistic antitumor effect, compared with either antibody alone. When examining T infiltration after treatment, we also found that combination therapy induced a lot more $CD8^+$ T cell infiltration in the tumor tissues than either antibody alone. Thus, we believe that combination therapy with endosialin antibody may provide a new option to overcome patients' resistance to PD-1 blockade in clinic.

Our study also has some limitations. For example, during the data analysis of scRNA-seq, we found that we only got relatively clear information about the immune cells in the tumors of EN^{KO} and WT mice while we did not get enough amount of CAFs to analyze their phenotype, which might be caused by the sample processing process. Thus, we could not conclude whether endosialin-positive CAFs belong to any specific CAF subcluster, as has been classified as myofibroblastic CAFs (myCAFs), inflammatory CAFs (iCAFs) or antigen-presenting CAFs (apCAFs).[52] However, according to our analysis of TCGA database, we found that endosialin was highly associated with extracellular structure organization and ECM organization (online supplemental figure 4A), indicating that they are more likely to be myCAFs. Yet we could not rule out the possibility that endosialin-positive CAFs may convert from iCAFs to myCAFs during tumor progression. More studies are needed to make it clear. In addition, during our study, we found that besides the increased infiltration of $CD8^+$ T cells, the number of MDSCs decreased in the tumor tissue of EN^{KO} mice than in WT mice. Whether endosialin may directly regulate the recruitment of MDSCs and the detailed mechanism is not known, further studies are also needed to make it clear. Furthermore, in our previous study in renal cell carcinoma (RCC), we found that endosialin-positive TDPs also could inhibit $CD8^+$ T cell infiltration to promote RCC progression, whether they also use similar mechanisms to exclude $CD8^+$ T cells also deserve further investigation.[53]

In conclusion, in this study, we demonstrate that endosialin-positive CAFs may promote HCC progression by suppressing $CD8^+$ T cell infiltration. We also demonstrate that endosialin is an effective target for HCC treatment, and combination therapy with endosialin antibody and PD-1 antibody provides a more effective therapeutic strategy, which may also overcome the resistance to PD-1 antibody.

Contributors LG and TL for acquisition, analysis and interpretation of data, statistical analysis and drafting of the manuscript. YL and HS for technical and material support. JZ and KZ for bioinformatic analysis and schematic image drawing. SL, XW, FN and SD for data analysis and constructive discussion. DH for reagent and material preparation. FY, WQ and WW for study concept and design, analysis and interpretation of data, revision of the manuscript, funding acquisition and study supervision. WW is the guarantor for this study. All authors read and approved the final manuscript.

Funding This study was supported by the National Natural Science Foundation of China (No. 82220108004; 82173204; 82203633; 82202933), the Innovation Capability Support Program of Shaanxi (2023-CX-TD-72; 2021TD-39; 2020PT-021), the Natural Science Basic Research Program of Shaanxi (2022JZ-62), and the open project program of the State Key Laboratory of Holistic Integrative Management of Gastrointestinal Cancers and National Clinical Research Center for Digestive Diseases (Fourth Military Medical University) (CBSKL2022ZDKF10).

Competing interests No, there are no competing interests.

Patient consent for publication Consent obtained directly from patient(s).

Ethics approval This study was approved by the Ethics Committee of Xijing Hospital, Fourth Military Medical University (approval No. KY20233429-1) and Medical and Experimental Animal Ethics Committee of Northwestern Polytechnical University (approval no. 202302016). All participants provided written informed consent. All experiments were carried out in accordance with the Code of Ethics of the World Medical Association (Declaration of Helsinki).

Provenance and peer review Not commissioned; externally peer reviewed.

Data availability statement Data are available on reasonable request.

ORCID iDs
Lunbiao Gan http://orcid.org/0009-0009-4394-0565
Tong Lu http://orcid.org/0000-0001-5691-9209
Yu Lu http://orcid.org/0009-0003-1548-9339
Hongtao Song http://orcid.org/0009-0007-4113-7432
Jiayu Zhang http://orcid.org/0000-0002-6898-6844
Keying Zhang http://orcid.org/0000-0002-4615-1782
Shiqi Lu http://orcid.org/0000-0001-7168-7813
Xinjie Wu http://orcid.org/0009-0000-2392-1994
Fengze Nie http://orcid.org/0009-0001-0360-3128
Sijia Di http://orcid.org/0009-0004-1590-6486
Donghui Han http://orcid.org/0000-0002-3742-4355
Fa Yang http://orcid.org/0009-0004-9259-0403
Weijun Qin http://orcid.org/0000-0002-7509-7164
Weihong Wen http://orcid.org/0000-0003-4739-4871

REFERENCES

1 Sung H, Ferlay J, Siegel RL, *et al*. Global Cancer Statistics 2020: GLOBOCAN Estimates of Incidence and Mortality Worldwide for 36 Cancers in 185 Countries. *CA Cancer J Clin* 2021;71:209–49.
2 Villanueva A. Hepatocellular Carcinoma. *N Engl J Med* 2019;380:1450–62.

3 Llovet JM, Kelley RK, Villanueva A, *et al*. Hepatocellular carcinoma. *Nat Rev Dis Primers* 2021;7:6.
4 Bejarano L, Jordão MJC, Joyce JA. Therapeutic Targeting of the Tumor Microenvironment. *Cancer Discov* 2021;11:933–59.
5 Affo S, Yu L-X, Schwabe RF. The Role of Cancer-Associated Fibroblasts and Fibrosis in Liver Cancer. *Annu Rev Pathol Mech Dis* 2017;12:153–86.
6 Baglieri J, Brenner DA, Kisseleva T. The Role of Fibrosis and Liver-Associated Fibroblasts in the Pathogenesis of Hepatocellular Carcinoma. *Int J Mol Sci* 2019;20:1723.
7 Mao X, Xu J, Wang W, *et al*. Crosstalk between cancer-associated fibroblasts and immune cells in the tumor microenvironment: new findings and future perspectives. *Mol Cancer* 2021;20:131.
8 Sahai E, Astsaturov I, Cukierman E, *et al*. A framework for advancing our understanding of cancer-associated fibroblasts. *Nat Rev Cancer* 2020;20:174–86.
9 Yin Z, Dong C, Jiang K, *et al*. Heterogeneity of cancer-associated fibroblasts and roles in the progression, prognosis, and therapy of hepatocellular carcinoma. *J Hematol Oncol* 2019;12:101.
10 Zhang J, Gu C, Song Q, *et al*. Identifying cancer-associated fibroblasts as emerging targets for hepatocellular carcinoma. *Cell Biosci* 2020;10:127.
11 Chen X, Song E. Turning foes to friends: targeting cancer-associated fibroblasts. *Nat Rev Drug Discov* 2019;18:99–115.
12 Biffi G, Oni TE, Spielman B, *et al*. IL1-Induced JAK/STAT Signaling Is Antagonized by TGFβ to Shape CAF Heterogeneity in Pancreatic Ductal Adenocarcinoma. *Cancer Discov* 2019;9:282–301.
13 Cogliati B, Yashaswini CN, Wang S, *et al*. Friend or foe? The elusive role of hepatic stellate cells in liver cancer. *Nat Rev Gastroenterol Hepatol* 2023;20:647–61.
14 Chen Y, McAndrews KM, Kalluri R. Clinical and therapeutic relevance of cancer-associated fibroblasts. *Nat Rev Clin Oncol* 2021;18:792–804.
15 Christian S, Ahorn H, Koehler A, *et al*. Molecular cloning and characterization of endosialin, a C-type lectin-like cell surface receptor of tumor endothelium. *J Biol Chem* 2001;276:7408–14.
16 Christian S, Winkler R, Helfrich I, *et al*. Endosialin (Tem1) is a marker of tumor-associated myofibroblasts and tumor vessel-associated mural cells. *Am J Pathol* 2008;172:486–94.
17 Rouleau C, Curiel M, Weber W, *et al*. Endosialin protein expression and therapeutic target potential in human solid tumors: sarcoma versus carcinoma. *Clin Cancer Res* 2008;14:7223–36.
18 Rouleau C, Smale R, Fu Y-S, *et al*. Endosialin is expressed in high grade and advanced sarcomas: evidence from clinical specimens and preclinical modeling. *Int J Oncol* 2011;39:73–89.
19 Teicher BA. CD248: A therapeutic target in cancer and fibrotic diseases. *Oncotarget* 2019;10:993–1009.
20 Lu S, Gan L, Lu T, *et al*. Endosialin in Cancer: Expression Patterns, Mechanistic Insights, and Therapeutic Approaches. *Theranostics* 2024;14:379–91.
21 Yang F, Wei Y, Han D, *et al*. Interaction with CD68 and Regulation of GAS6 Expression by Endosialin in Fibroblasts Drives Recruitment and Polarization of Macrophages in Hepatocellular Carcinoma. *Cancer Res* 2020;80:3892–905.
22 Castelló-Cros R, Cukierman E. Stromagenesis during tumorigenesis: characterization of tumor-associated fibroblasts and stroma-derived 3D matrices. *Methods Mol Biol* 2009;522:275–305.
23 Anders S, Pyl PT, Huber W. HTSeq--a Python framework to work with high-throughput sequencing data. *Bioinformatics* 2015;31:166–9.
24 Yan B, Ouyang Q, Zhao Z, *et al*. Potent killing of HBV-related hepatocellular carcinoma by a chimeric protein of anti-HBsAg single-chain antibody and truncated Bid. *Biomaterials* 2013;34:4880–9.
25 Xu Z, Chen D, Hu Y, *et al*. Anatomically distinct fibroblast subsets determine skin autoimmune patterns. *Nature New Biol* 2022;601:118–24.
26 Klement JD, Redd PS, Lu C, *et al*. Tumor PD-L1 engages myeloid PD-1 to suppress type I interferon to impair cytotoxic T lymphocyte recruitment. *Cancer Cell* 2023;41:620–36.
27 Dangaj D, Bruand M, Grimm AJ, *et al*. Cooperation between Constitutive and Inducible Chemokines Enables T Cell Engraftment and Immune Attack in Solid Tumors. *Cancer Cell* 2019;35:885–900.
28 Filliol A, Saito Y, Nair A, *et al*. Opposing roles of hepatic stellate cell subpopulations in hepatocarcinogenesis. *Nature New Biol* 2022;610:356–65.
29 Zaki MYW, Alhasan SF, Shukla R, *et al*. Sulfatase-2 from Cancer Associated Fibroblasts: An Environmental Target for Hepatocellular Carcinoma? *Liver Cancer* 2022;11:540–57.
30 Song M, He J, Pan Q-Z, *et al*. Cancer-Associated Fibroblast-Mediated Cellular Crosstalk Supports Hepatocellular Carcinoma Progression. *Hepatology* 2021;73:1717–35.
31 Zhu G-Q, Tang Z, Huang R, *et al*. CD36$^+$ cancer-associated fibroblasts provide immunosuppressive microenvironment for hepatocellular carcinoma via secretion of macrophage migration inhibitory factor. *Cell Discov* 2023;9:25.
32 Xiong S, Wang R, Chen Q, *et al*. Cancer-associated fibroblasts promote stem cell-like properties of hepatocellular carcinoma cells through IL-6/STAT3/Notch signaling. *Am J Cancer Res* 2018;8:302–16.
33 Liu J, Chen S, Wang W, *et al*. Cancer-associated fibroblasts promote hepatocellular carcinoma metastasis through chemokine-activated hedgehog and TGF-β pathways. *Cancer Lett* 2016;379:49–59.
34 Mano Y, Yoshio S, Shoji H, *et al*. Bone morphogenetic protein 4 provides cancer-supportive phenotypes to liver fibroblasts in patients with hepatocellular carcinoma. *J Gastroenterol* 2019;54:1007–18.
35 Liu M, Zhou J, Liu X, *et al*. Targeting monocyte-intrinsic enhancer reprogramming improves immunotherapy efficacy in hepatocellular carcinoma. *Gut* 2020;69:365–79.
36 Zhen Z, Tang W, Wang M, *et al*. Protein Nanocage Mediated Fibroblast-Activation Protein Targeted Photoimmunotherapy To Enhance Cytotoxic T Cell Infiltration and Tumor Control. *Nano Lett* 2017;17:862–9.
37 Loeffler M, Krüger JA, Niethammer AG, *et al*. Targeting tumor-associated fibroblasts improves cancer chemotherapy by increasing intratumoral drug uptake. *J Clin Invest* 2006;116:1955–62.
38 Lang J, Zhao X, Qi Y, *et al*. Reshaping Prostate Tumor Microenvironment To Suppress Metastasis *via* Cancer-Associated Fibroblast Inactivation with Peptide-Assembly-Based Nanosystem. *ACS Nano* 2019;13:12357–71.
39 Hofheinz R-D, al-Batran S-E, Hartmann F, *et al*. Stromal Antigen Targeting by a Humanised Monoclonal Antibody: An Early Phase II Trial of Sibrotuzumab in Patients with Metastatic Colorectal Cancer. *Oncol Res Treat* 2003;26:44–8.
40 Roberts EW, Deonarine A, Jones JO, *et al*. Depletion of stromal cells expressing fibroblast activation protein-α from skeletal muscle and bone marrow results in cachexia and anemia. *J Exp Med* 2013;210:1137–51.
41 Llovet JM, Castet F, Heikenwalder M, *et al*. Immunotherapies for hepatocellular carcinoma. *Nat Rev Clin Oncol* 2022;19:151–72.
42 Qin S, Ren Z, Meng Z, *et al*. Camrelizumab in patients with previously treated advanced hepatocellular carcinoma: a multicentre, open-label, parallel-group, randomised, phase 2 trial. *Lancet Oncol* 2020;21:571–80.
43 El-Khoueiry AB, Sangro B, Yau T, *et al*. Nivolumab in patients with advanced hepatocellular carcinoma (CheckMate 040): an open-label, non-comparative, phase 1/2 dose escalation and expansion trial. *Lancet* 2017;389:2492–502.
44 Finn RS, Ryoo B-Y, Merle P, *et al*. Pembrolizumab As Second-Line Therapy in Patients With Advanced Hepatocellular Carcinoma in KEYNOTE-240: A Randomized, Double-Blind, Phase III Trial. *J Clin Oncol* 2020;38:193–202.
45 Finn RS, Qin S, Ikeda M, *et al*. Atezolizumab plus Bevacizumab in Unresectable Hepatocellular Carcinoma. *N Engl J Med* 2020;382:1894–905.
46 Kelley RK, Sangro B, Harris W, *et al*. Safety, Efficacy, and Pharmacodynamics of Tremelimumab Plus Durvalumab for Patients With Unresectable Hepatocellular Carcinoma: Randomized Expansion of a Phase I/II Study. *J Clin Oncol* 2021;39:2991–3001.
47 Greten TF, Villanueva A, Korangy F, *et al*. Biomarkers for immunotherapy of hepatocellular carcinoma. *Nat Rev Clin Oncol* 2023;20:780–98.
48 Jiang X, Wang J, Deng X, *et al*. Role of the tumor microenvironment in PD-L1/PD-1-mediated tumor immune escape. *Mol Cancer* 2019;18:10.
49 Pei L, Liu Y, Liu L, *et al*. Roles of cancer-associated fibroblasts (CAFs) in anti- PD-1/PD-L1 immunotherapy for solid cancers. *Mol Cancer* 2023;22:29.
50 Raskov H, Orhan A, Christensen JP, *et al*. Cytotoxic CD8+ T cells in cancer and cancer immunotherapy. *Br J Cancer* 2021;124:359–67.
51 Huang Q, Wu X, Wang Z, *et al*. The primordial differentiation of tumor-specific memory CD8$^+$ Tcells as bona fide responders to PD-1/PD-L1 blockade in draining lymph nodes. *Cell* 2022;185:4049–66.
52 Caligiuri G, Tuveson DA. Activated fibroblasts in cancer: Perspectives and challenges. *Cancer Cell* 2023;41:434–49.
53 Lu T, Zhang J, Lu S, *et al*. Endosialin-positive tumor-derived pericytes promote tumor progression through impeding the infiltration of CD8$^+$ T cells in clear cell renal cell carcinoma. *Cancer Immunol Immunother* 2023;72:1739–50.